

AN EXERGY ANALYSIS FOR OVERALL HIDDEN LOSSES OF ENERGY IN SOLAR WATER HEATER

Sathyakala Ponnusamy^{*1}, *Sai Sundara Krishnan Gangadharan*² and *Balaji Kalaiarasu*³

^{*1}Department of Mathematics, PSG College of Technology, Coimbatore-641 004, Tamilnadu, India

²Department of Applied Mathematics & Computational Sciences, PSG College of Technology, Coimbatore-641004, Tamilnadu, India

³Department of Mechanical Engineering, Amrita School of Engineering, Ettimadai, Coimbatore-641112, Tamilnadu, India

* Corresponding author; E-mail: psl.maths@psgtech.ac.in

This study investigates the hidden thermal losses of glass plate, collector plate, water pipe and storage tank of solar water heater in the process of energy conversion. The present non-conventional energy methods are insufficient, whereas the exergy analysis provides a remarkable solution. Thus, employing the exergy analysis, entropy generation, exergy destruction and exergy efficiency of each subsystem of solar water heater are computed. The obtained results showed that the entropy generation and exergy destruction are high during the heat transfer in each subsystem. Henceforth, the existing solar water heater design is modified placing hexagonal honeycomb structure between the glass plate and the collector plate and also water pipe is insulated to trap huge amount of solar energy. The proposed design exhibits improved exergy efficiency when compared with the existing model, which enhances the performance of the system.

Key words: Solar water heater, Energy balance, Exergy destruction, Exergy efficiency

1. Introduction

The world energy demand is rapidly rising due to the high-speed growing of technology. The increased depletion of fossil fuels has led to the quest for alternative fuel resources of energy. Currently, solar energy is the most accessible and inexhaustible form of energy, which involves considerable attention for generating heat and electricity. Solar Water Heater (SWH) is the popular source of solar energy utilization because of technological feasibility and economic attraction, when compared to other kinds of solar energy utilization. Thus, to optimize solar system design parameters and process, the second law of thermodynamics (exergy efficiency) is necessary [1].

Suzuki A compared an evacuated tubular collector and a flat-plate collector by assuming a fixed overall heat loss coefficient, and showed that they both have nearly equal potential in exergy gain [1]. Dutta Gupta et al., carried out a thermal and exergy investigation of solar collector by assuming an invariable overall heat loss coefficient and fluid inlet temperature [2]. Luminosu, I, Fara. L proved that the collector's overall exergy efficiency depends upon fluid flow rate plus the collector area [3]. Farahat et al., had developed an exergetic optimization of a flat plate solar collector, to determine the optimal performance and design parameters of the solar to a thermal energy conversion system [4].

Farzad Jafarkazemi et.al., showed experimentally and theoretically, better exergetic performance as an effect of rising water inlet temperature along with decreasing water mass flow rate [5]. Zhong Ge et al., had proposed exergy model for the study of flat plate solar collectors by taking

into account a non- uniformity in the temperature distribution along the absorber plate [6]. Gopal Sivaraman et.al., proposed that the flat plate bend tube solar collector employs additional energy which in turn enhances the outlet water temperature [7]. Malvi C S et al., experimentally pointed out the heat removal factor F_R is highly influenced by the systems fin efficiency and its value does not increases for the mass flow rate beyond 4 kg/h [8]. Orlando Montoya-Marquez et al., showed that the heat removal factor F_R linearly increases with 14.5% change for inclinations from horizontal to vertical [9].

K.G.T. Hollands presented a simplified analysis of four aspects of squared honeycomb array and pointed the significance of wall thickness of honeycomb [10]. Atish Mozumder et al., found the performance of the system with the honeycomb is enhanced than the one without the honeycomb when the incident angle of the solar radiation is within 20° [11]. A.H. Abdullah et al., revealed the use of honeycomb in solar collectors has a benefit of reducing the top heat loss and also the penalty of decreasing the optical efficiency [12].

The above studies recognized the importance of utilization of renewable energy in SWH, optimization of flat plate collector efficiency, energy conversion and exergy analysis. This motivated the present study to focus on the experimental work to extract hidden losses by accounting exergy destruction in each subsystem of the SWH using the second law of thermodynamics.

2. Thermodynamic analysis of solar water heater

The energy, exergy and entropy [13] for each subsystem of the SWH are analyzed by considering the output at each stage as input for the subsequent stages with the assumptions: (i) All of the correlations have been written in one dimensional steady state and steady flow condition, (ii) Iterative procedure is employed to estimate the top loss coefficient with the range of variables in Tab.1, (iii) The solar collector's heat transfer coefficient and agent fluid properties are taken as constants and (iv) The exergy loss caused by the ducts' pressure drop is negligible.

2.1. Glass plate

The glass plate [11] in Fig. 1 reduces convective and radiative heat losses from the absorber, to transmit incident solar radiation to the absorber plate with minimum loss and to protect the absorber plate from the effects of climatic change.

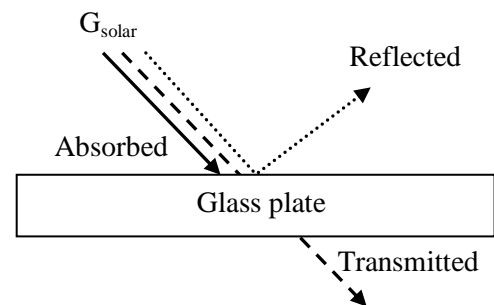


Figure 1. Glass plate

2.1.1. Energy Absorption

The heat energy input rate in the glass plate from the solar energy is

$$\dot{Q}_{in,gp} = \alpha_s G_{solar} A_p \quad (1)$$

Heat transfer loss rate from the glass plate occurs in two modes, namely radiation and convection and is given by

$$\dot{Q}_{l,gp} = \varepsilon \sigma A_p (T_{sf}^4 - T_{air}^4) + h_{conv} A_p (T_{sf} - T_{air}) \quad (2)$$

The convective heat transfer coefficient is calculated based on the correlation between Rayleigh(Ra_L) and Nusselt number(Nu_L). The rate of heat energy absorbed by the glass plate is

$$\dot{Q}_{abs,gp} = \dot{Q}_{in,gp} - \dot{Q}_{l,gp} \quad (3)$$

The heat energy absorbed by the glass plate will be the input for the honeycomb structure.

2.1.2. Entropy Generation

The increase of entropy principle states that the entropy can only be created. At steady state, entropy change is zero. The rate of Entropy generation within the glass plate is calculated by

$$\dot{S}_{gen,gp} = \left(\frac{\dot{Q}_{l,gp}}{T_{air}} \right) \quad (4)$$

2.1.3. Exergy Destruction and Exergy efficiency

The loss of available energy due to the conception of entropy in irreversible processes of the glass plate is articulated by exergy. The exergy destruction of the glass plate is

$$\dot{X}_{des,gp} = T_o \dot{S}_{gen,gp} \quad (5)$$

$$\eta_{ex,gp} = 1 - \frac{\dot{X}_{des,gp}}{\dot{X}_{in,gp}} \quad (6)$$

2.2. Honeycomb Structure

Each subsystem of the SWH is analyzed to determine the areas of major heat losses. Although, solar collector transfers the solar energy into useful heat in a competent way, the efficiency of solar collector is low due to heat dissipation. To reduce the exergy destruction two modifications to the design were adapted specifically, honeycomb structure and water pipe insulation. The heat loss by radiation forms an essential fraction of total heat loss from the top surface of the absorber plate. A honeycomb layer is sited between the collector and glass cover plate which acts as convection suppression device that reduces the heat loss and increases the collector's efficiency.

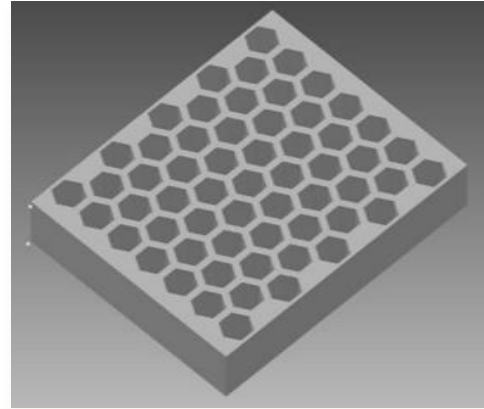


Figure. 2. 3-D view of Honeycomb structure

2.2.1. Energy Absorption

The energy balance for honeycomb structure is given by

$$\dot{Q}_{in,hc} - \dot{Q}_{l,hc} = \dot{Q}_{out/abs,hc} \quad (7)$$

Here $\dot{Q}_{in,hc} = \dot{Q}_{abs,gp}$, as the output of previous stage is considered as input of present stage. Heat transfer loss from the honeycomb devices occur in three forms, namely natural convection, radiation and conduction heat transfer through honeycomb walls. The conventional heat loss is

$$\dot{Q}_{l,hc} = U_{hc} A_p (T_{1,hc} - T_{2,hc}) \quad (8)$$

where $T_{1,hc}, T_{2,hc}$ are temperature differences of two faces of honeycomb panel.

The overall heat transfer coefficients U_{hc} across the panel is given by

$$U_{hc} = h_a + h_r + h_c \quad (9)$$

The natural heat transfer coefficient h_a , based on Nusselt number is

$$h_a = (Nu_L K_a) / d \quad (10)$$

Also, if the faces of the honeycomb are grey and have emissivity's ϵ_1 and ϵ_2 and reflectance's ρ_1 and ρ_2 , the radiant heat flux h_r between the two faces [14] is

$$h_r = \frac{F_1 \sigma (T_{1,hc}^4 - T_{2,hc}^4)}{(T_{1,hc} - T_{2,hc})} \quad (11)$$

$$\frac{1}{F_1} = \frac{1}{F} + \frac{\rho_1}{\epsilon_1} + \frac{\rho_2}{\epsilon_2} \quad (12)$$

Here F, F_1 are the equivalent form factors between the two faces [14]. Then the mean heat flux h_c for hexagonal array in Fig. 2 might be is defined as

$$h_c = \frac{3\delta K_H (T_1 - T_2)}{wd} \quad (13)$$

2.3. Flat Collector Plate

A flat plate solar collector in Fig. 3 carries out the three effective mechanisms: (i) Absorbs the utmost potential amount of solar irradiance; (ii) Conduct heat in the direction of the working fluid at least temperature difference; (iii) Drop smallest amount of heat back to the surroundings.



Figure 3. Experimental setup

2.3.1. Energy Absorption

The useful heat gain by the working fluid is

$$\dot{Q}_{cp} = \dot{m} C_p (T_{out,cp} - T_{in,cp}) \quad (14)$$

There is no mass flow in the absorber plate under steady state. Also, the heat energy absorbed by the honeycomb panel will be the input for the collector plate. By considering, overall heat loss coefficient U_l , the Hottel–Whillier equation for useful heat collected per unit area [15] is

$$\dot{Q}_{cp} = A_p F_R [S_r - U_l (T_{in} - T_{air})] \quad (15)$$

Based on the three components, the top loss coefficient U_t , the bottom loss coefficient U_s and the side loss coefficient U_l, U_l given by

$$U_l = U_t + U_b + U_s \quad (16)$$

The heat removal factor is defined as

$$F_R = \frac{\dot{m} C_p}{U_l A_p} \left[1 - \exp \left\{ \frac{F' U_l A_p}{\dot{m} C_p} \right\} \right] \quad (17)$$

In equation (15), the radiation absorbed flux by unit area of the absorber plate is defined as

$$S_r = (\tau\alpha) I_T \quad (18)$$

2.3.2. Entropy Generation

The rate of change of the entropy generated in the collector plate is given by

$$\dot{S}_{gen,cp} = \frac{\dot{Q}_{l,cp}}{T_{air}} \quad (19)$$

The heat loss from the collector plate in terms of overall loss coefficient is expressed as

$$\dot{Q}_{l,cp} = U_l A_p (T_p - T_{air}) \quad (20)$$

2.3.3. Exergy Destruction and Exergy efficiency

The general form of exergy balance of the collector plate is,

$$\dot{X}_{in} + \dot{X}_{sd} + \dot{X}_{out} + \dot{X}_{lk} + \dot{X}_{des} = 0 \quad (21)$$

where \dot{X}_{in} , \dot{X}_{sd} , \dot{X}_{out} , \dot{X}_{lk} and \dot{X}_{des} are the inlet, stored, outlet, leakage and destroyed exergy rate respectively. The inlet exergy rate includes the inlet exergy rate with fluid flow and the absorbed solar radiation exergy rate. The inlet exergy rate with fluid flow is

$$\dot{X}_{in,m} = \dot{m} C_p \left(T_{in,cp} - T_{air} - T_{air} \ln \left(\frac{T_{in,cp}}{T_{air}} \right) \right) \quad (22)$$

Assuming the sun as an infinite thermal source, the absorbed solar radiation exergy rate is [16]

$$\dot{X}_{in,r} = \eta_o I_T A_p \left(1 - \frac{T_{air}}{T_{sun}} \right) \quad (23)$$

The summing up of equation (22) and (23) will result in total inlet exergy rate of the solar collector. The stored exergy rate is null at steady state conditions. The outlet exergy rate includes only the exergy rate of outlet fluid flow.

$$\dot{X}_{out,m} = -\dot{m} C_p \left(T_{out,cp} - T_{air} - T_{air} \ln \left(\frac{T_{out,cp}}{T_{air}} \right) \right) \quad (24)$$

The leakage exergy rate caused by heat leakage rate from the absorber plate to the environment [2] is

$$\dot{X}_{lk} = -U_l A_p (T_p - T_{air}) \left(1 - \frac{T_{air}}{T_p} \right) \quad (25)$$

The destroyed exergy rate comprises two expressions: the first is caused by the temperature difference between the absorber plate surface and the sun [2], the second is caused by the temperature difference between the absorber plate surface and the agent fluid [1]. Correspondingly the equations are

$$\dot{X}_{des,\Delta T_s} = -\eta_o I_T A_p T_{air} \left(\frac{1}{T_p} - \frac{1}{T_{sun}} \right) \quad (26)$$

$$\dot{X}_{des,\Delta T_f} = -\dot{m} C_p T_{air} \left(\ln \left(\frac{T_{out,cp}}{T_{in,cp}} \right) - \left(\frac{T_{out,cp} - T_{in,cp}}{T_p} \right) \right) \quad (27)$$

Substituting Eqs. (22) - (27) into Eq. (21) and considering the exergy efficiency definition, the second law efficiency is derived [2], [3] and [16].

$$\eta_{ex,cp} = 1 - \left\{ (1 - \eta_0) + \frac{\eta_0 T_{air} \left(\frac{1}{T_p} - \frac{1}{T_{sun}} \right)}{\left(1 - \frac{T_{air}}{T_{sun}} \right)} + \frac{U_l (T_p - T_{air}) \left(1 - \frac{T_{air}}{T_p} \right)}{I_T \left(1 - \frac{T_{air}}{T_{sun}} \right)} + \frac{\dot{m} C_p T_{air} \left(\ln \left(\frac{T_{out,cp}}{T_{in,cp}} \right) - \left(\frac{T_{out,cp} - T_{in,cp}}{T_p} \right) \right)}{I_T A_p \left(1 - \frac{T_{air}}{T_{sun}} \right)} \right\} \quad (28)$$

2.4. Water Pipe

The hot water pipe of the collector is assumed to be a closed system for energy and exergy equilibrium analysis, with constant properties. The heat energy from collector plate is carried out by water flowing inside the pipe.

2.4.1. Energy absorption without insulation

The energy balance equation by considering the mass flow inside the pipe, is given by

$$\dot{Q}_{in,wp} + \dot{m} \theta_{in,wp} = \dot{Q}_{out,wp} + \dot{m} \theta_{out,wp} \quad (29)$$

$$\dot{m} \theta_{in,wp} = \dot{m}_{in} \left(h_{in} + \frac{C_{in}^2}{2} + gZ_{in} \right)_{wp} \quad (30)$$

where, θ is the energy associated with the flowing fluid, h is the enthalpy, Z is the vertical height from the reference, g is acceleration due to gravity and C is the velocity of the fluid medium.

$$\dot{m} \theta_{out,wp} = \dot{m}_{out} \left(h_{out} + \frac{C_{out}^2}{2} + gZ_{out} \right)_{wp} \quad (31)$$

In the pipe flow, kinetic energy in and out, potential energy in and out are equal and can be neglected.

2.4.2. Energy absorption with insulation

The amount of heat loss is due to convection losses in the connecting pipes between the absorber plate and storage tank. Since the temperature of the fluid flowing inside the pipes is higher than the surrounding temperature, there will be huge amount of heat loss to the surroundings. By selecting suitable insulating material for the connecting pipes, heat loss can be reduced. This reduces the exergy destruction and increases the second law efficiency of the system to a limit. The proposed insulating material is glass wool in Fig. 4 due to its low cost and good insulating properties. The energy balance for the insulated water pipe is

$$\dot{Q}_{in,wp} = \dot{m} \theta_{out,wp} - \dot{m} \theta_{in,wp} \quad (32)$$

2.4.3. Entropy Generation



Figure 4. Insulation of pipes using Glass wool

The heat loss rate in the water pipe without insulation is evaluated as

$$\dot{Q}_{l,wp} = \frac{L\pi(T_f - T_{air})}{\frac{\ln(\frac{D_o}{D_i})}{2k} + \frac{1}{h_{sf}D_o}} \quad (33)$$

The heat loss rate in the water pipe with insulation is evaluated as

$$\dot{Q}_{l,wp} = \frac{L\pi(T_f - T_{air})}{\frac{\ln(\frac{D_s}{D_i})}{2k} + \frac{1}{h_{sf}D_s}} \quad (34)$$

The rate of change of the entropy generated in the water pipe is given by

$$\dot{S}_{gen,wp} = \frac{\dot{Q}_{l,wp}}{T_{air}} \quad (35)$$

2.5. Storage Tank

A storage tank in Fig. 5 is the main component of the SWH to be considered for sizing. Principle of storage tank is to provide: Generous amount of hot water storage; a reasonable price to build, and a long boring life.

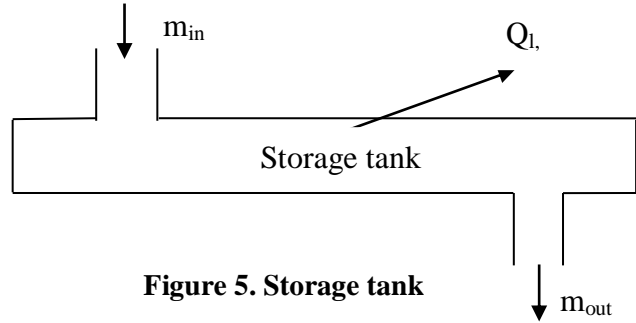


Figure 5. Storage tank

2.5.1. Energy absorption

The useful heat gain from storage tank to end user is expressed as

$$\dot{Q}_{st} = \dot{m}C_p(T_{out,cp} - T_{t,st}) \quad (36)$$

2.5.2. Entropy Generation

The heat loss rate in the storage tank is evaluated as

$$\dot{Q}_{l,st} = \frac{(T_{t,st} - T_{air})}{\left(\frac{1}{\pi h_{sf} D_{st} H_{st}}\right)} \quad (37)$$

where D_{st} , H_{st} denotes the diameter and height of the storage tank respectively. The rate of change of entropy generated in the storage tank is given by

$$\dot{S}_{gen,st} = \frac{\dot{Q}_{l,st}}{T_{air}} \quad (38)$$

2.5.3. Exergy Destruction and Exergy Efficiency

The exergy rate from collector plate to storage tank is calculated as

$$\dot{X}_{cp-st} = \dot{m}C_p(T_{out,cp} - T_{t,st}) - \dot{m}T_{air}C_p \ln\left(\frac{T_{out,cp}}{T_{t,st}}\right) \quad (39)$$

The exergy rate from storage tank to end user is given by

$$\dot{X}_{st-end} = \dot{m}C_p \left[\left(\frac{T_{t,cp} + T_{b,st}}{2} - T_{air} \right) - T_{air} \left(\ln \left(\frac{T_{t,st}}{T_{air}} \right) - 1 \right) - \frac{T_{b,st}T_{air}}{T_{t,st} - T_{b,st}} \ln \left(\frac{T_{t,st}}{T_{b,st}} \right) \right] \quad (40)$$

where $T_{b,st}$ is the temperature of the water at bottom of the storage tank. The exergy destruction is

$$\dot{X}_{des,st} = T_o * \dot{S}_{gen,st} \quad (41)$$

$$\eta_{ex,st} = 1 - \frac{\dot{X}_{des,st}}{\dot{X}_{in,st}} \quad (42)$$

3. Results and Discussion

Tab.1. represents the geometrical parameters of SWH and thermo-physical properties of agent fluid. Assuming one-dimensional heat flow and considering the thermal capacity and temperature drop across the glass cover, iterative procedure was employed to estimate the top loss coefficient.

Table 1. Environmental parameters and specifications of the SWH

| SWH parameters | Values |
|---|-------------------------------------|
| Mass flow rate of the working fluid \dot{m} | 0.002 kg/s |
| Heat Capacity of the fluid C_p | 4186 kJ/kg K |
| Type | Black paint header-riser flat plate |
| Outlet temperature T_{out} | 360 K |
| Glazing | Double glass |
| Agent fluid in flow ducts | Water |
| Adhesive resistance | Negligible |
| Length and width of the collector | 1.88 m × 0.98 m |
| Wind speed V_a | 25 m/s |
| Collector tilt β | 20° |
| Fluid inlet temperature T_{in} | 305 K |
| Ambient Temperature T_{air} | 300 K |
| Apparent Sun Temperature T_{sun} | 4350 K |
| Plate Thickness δ_p | 0.002 m |
| Optical Efficiency $\eta_o (= \tau\alpha)$ | 0.84 |
| Emissivity of the absorber plate ε_p | 0.92 |
| Emissivity of the covers ε_c | 0.88 |
| Glass covers distance $\delta_1 = \delta_2$ | 0.04 m |
| Thickness of back insulation δ_b | 0.08 m |
| Thickness of sides insulation δ_e | 0.04 m |
| Thermal conductivity of the absorber plate K_p | 384 W/m K |
| Thermal conductivity of the insulation K_i | 0.05 W/m K |
| Incident solar energy per unit area of the absorber plate I_T | 500 W/m ² |
| Tubes center to center distance W | 0.15 m |
| Inner diameter of the pipe D_i | 0.04 m |
| Outer diameter of the pipes D_o | 0.044 m |
| Fluid temperature at top of the storage tank $T_{t,st}$ | 343 K |
| Fluid temperature at bottom of the storage tank $T_{b,st}$ | 312 K |
| New outlet temperature of water from collector plate $T_{out,cp}$ | 362 K |
| New fluid temperature at top of the storage tank $T_{t,st}$ | 345 K |
| Diameter of the storage tank D_{st} | 1370 mm |
| Height of the storage tank H_{st} | 1465 mm |

An extensive exergy analysis has been carried out in each subsystem of SWH. Exergy efficiency in Tab. 2. is high for glass plate whereas for other subsystems it is drastically low, which makes a room for the researchers to examine modification in the system for the improvement in exergy efficiency.

Table 2. Exergy analysis of the existing model

| Components of SWH | Energy absorption \dot{Q}_{abs} [kW] | Entropy Generation \dot{S}_{gen} [$\frac{kW}{K}$] | Exergy Destruction \dot{X}_{des} [kW] | Exergy Efficiency η_{II} % |
|-----------------------------------|---|--|--|------------------------------------|
| Glass plate | 2.2599 | 0.646 | 0.193 | 92.101 |
| Collector plate without honeycomb | 0.461 | 1.689×10^{-3} | 0.504 | 5.181 |
| Water pipes without insulation | 0.0670 | 2.612×10^{-3} | 0.778 | 1.354 |
| Storage tank | 0.2595 | 0.01165 | 3.4726 | 1.280 |

To account the irreversibility in each subsystem, the present study customized a honeycomb structure placed between the glass and absorber plate to reduce the convective and radiation losses. It is observed that the exergy efficiency of collector plate has been slightly increased. However, the effects of honeycomb and pipe insulation are not showing much change in the exergy efficiency, but this change may conserve a lot of energy in the long run. Also, if there is any irreversibility in the system, it gets converted into useful work which leads to improvement of performance of the system. Tab. 3 shows the increase in the efficiency of each subsystem after converting the hidden losses into useful work.

Table 3. Exergy analysis of the modified model

| Components of SWH | Energy absorption \dot{Q}_{abs} [kW] | Entropy Generation \dot{S}_{gen} [$\frac{kW}{K}$] | Exergy Destruction \dot{X}_{des} [kW] | Exergy Efficiency η_{II} % |
|--------------------------------|---|--|--|------------------------------------|
| Glass plate | 2.2599 | 0.646 | 0.193 | 92.101 |
| Collector plate with Honeycomb | 0.4772 | 1.605×10^{-3} | 0.478 | 5.298 |
| Water pipes with insulation | 0.0921 | 5.861×10^{-4} | 0.175 | 1.914 |
| Storage tank | 0.2763 | 0.0112 | 3.3243 | 1.832 |

With the help of exergy analysis, the energy input and output are equated which gives a clear picture of the system, including hidden losses. The second law efficiency has been analyzed before and after the improvisation of energy efficiency. Fig. 6 illustrates that by reducing the losses in each subsystem, the exergy efficiency of the collector plate, water pipe and storage tank are increased from 5.181% to 5.298%, 1.354% to 1.914% and 1.280% to 1.832% respectively.

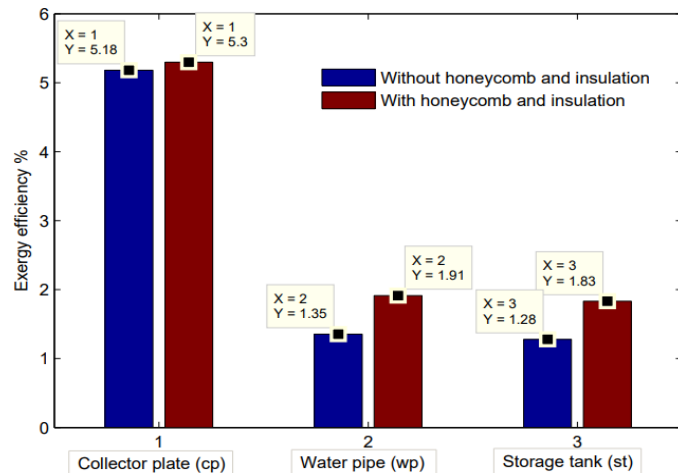


Figure 6. The variations of exergy efficiency between existing model and modified model.

Fig. 7 (a1) shows that the exergy efficiency and the collector plate area are positively correlated up to a maximum point for both the models, then the efficiency between the models coincides. Fig.7 (a2) demonstrates the increase in exergy efficiency progressively up to a specified inlet temperature and its decrease as inlet temperature increases. Thus, the exergy efficiency of the system is optimum up to a particular fluid temperature.

Fig. 8 (a1) and (a2) illustrates the variations of exergy efficiency as a function of collector plate

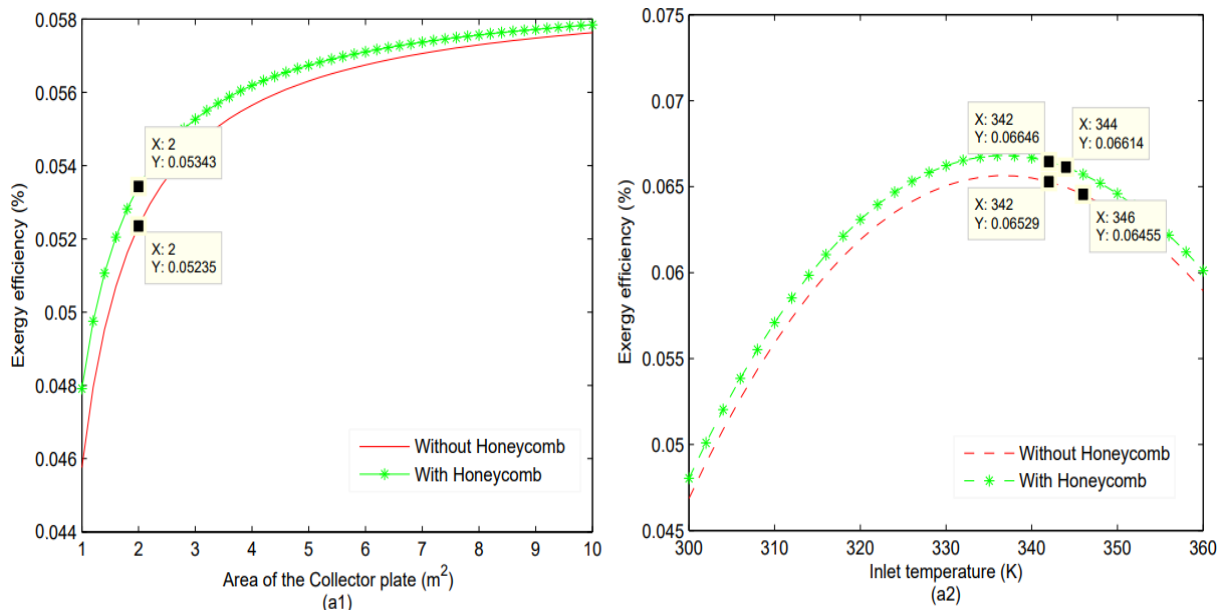


Figure 7. (a1) Area of the plate vs exergy efficiency, (a2) Inlet temperature vs exergy

area and mass flow rate of the agent fluid in three dimensional views. It is inferred that the exergy efficiency is maximum at fixed lower flow rate for the range of collector plate area. This is due to the effective transformation of energy from the collector plate to the agent fluid. The efficiency decreases gradually when the flow rate of the fluid is increased for the range of collector plate area.

Fig. 9 (a1) points that the exergy efficiency increases as the optical efficiency increases and the difference between the exergy efficiency of both the models are consistent with increase in optical

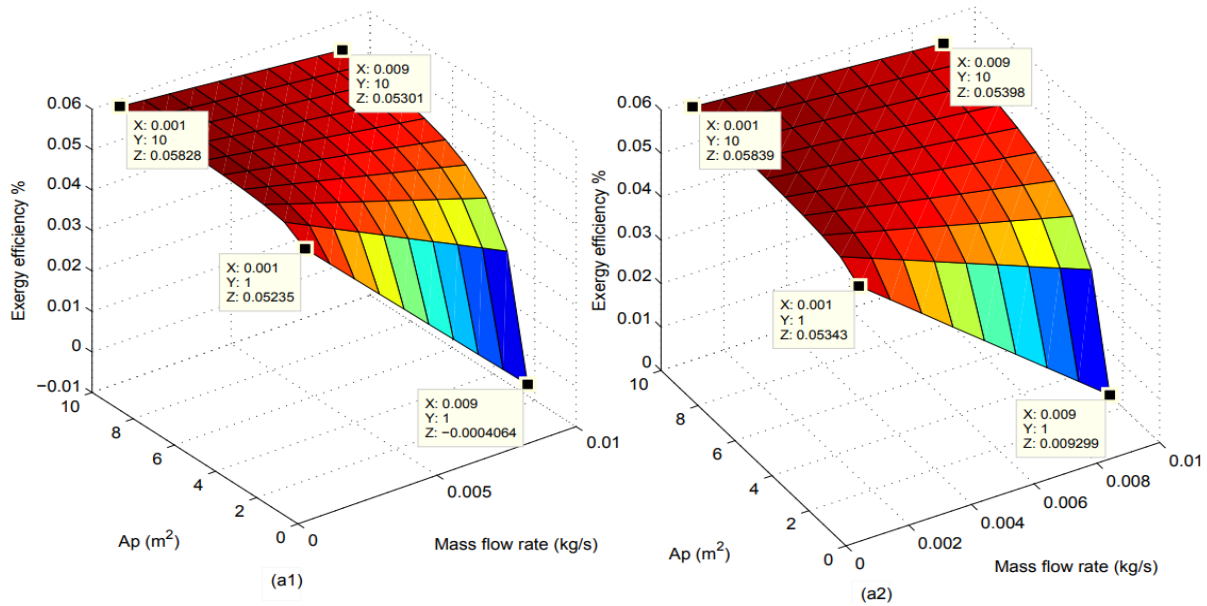


Figure 8. Variations of exergy efficiency according to mass flow rate and area of the plate: (a1) for the existing model, (a2) for the modified model

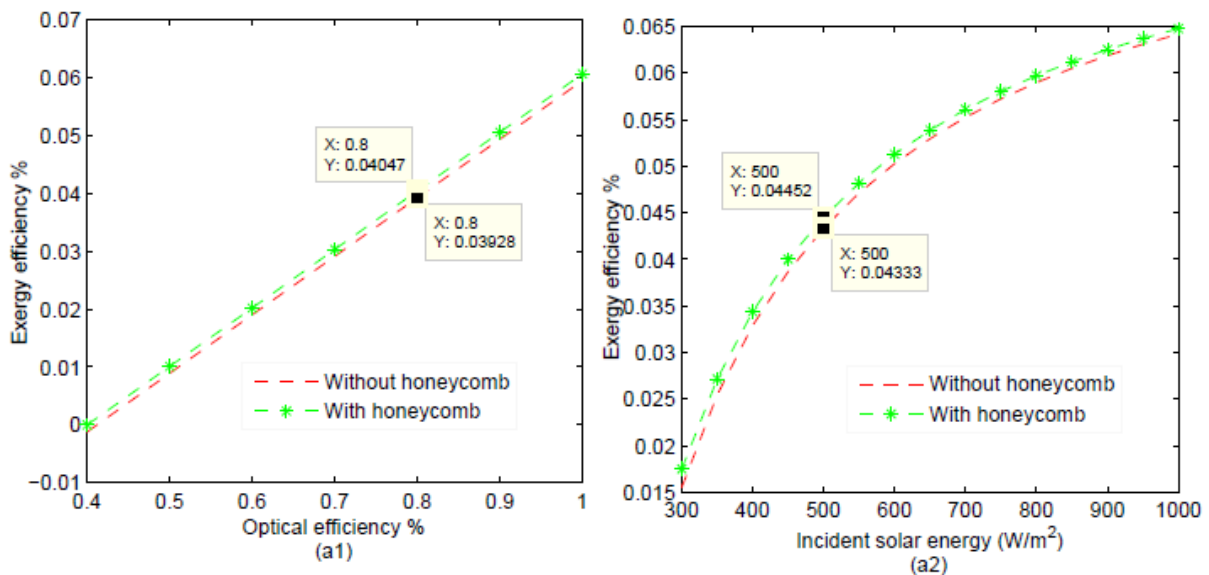


Figure 9 (a1). Exergy efficiency versus optical efficiency, (a2) Exergy efficiency versus incident solar energy per unit area of the flat plate collector

efficiency. Fig. 9 (a2) shows the effect of incident solar energy per unit area of the flat plate collector and exergy efficiency increases with respect to this parameter and the variation between the exergy efficiency of the existing model and modified model is reduced with increase in incident solar energy.

4. Conclusion and Future Scope

In this work, a solar water heater with flat plate collector was experimentally tested (i) with and without honeycomb structure inserted between glass plate and collector plate (ii) with and without insulated water pipe. Based on this study the following conclusions have been drawn:

Exergy efficiencies for the consecutive stages of solar water heater are calculated and the results of the entropy generation and exergy destruction are compared with both existing and modified model. The obtained results showed that the accuracy of the exergy efficiency of the collector plate, water pipe and storage tank are increased from 5.181% to 5.298%, 1.354% to 1.914% and 1.280% to 1.832% respectively. Though the impact of honeycomb structure and water pipe insulation is showing feeble variation in the exergy efficiency, this change may eventually preserve a lot of energy.

The graphical results showed that the exergy efficiency and the collector plate area are positively correlated. Also, increase in fluid inlet temperature, increases exergy efficiency up to a maximum point, beyond which they are negatively correlated. By increasing the optical efficiency, exergy efficiency increases and varies uniformly for both the models. Moreover, the obtained results showed a positive correlation between exergy efficiency and incident solar energy per unit area of the flat plate collector.

The exergy analysis presented in this paper can be extended to introduce the phase change material module of similar system, to establish the analysis of hidden losses. The future scope of the work is to carry out an exergoeconomic analysis to bring out the exergy cost which is useful for performing thermal analysis of any system.

This study concludes that any product which comes out through an exergy analysis designates the conservation of energy to a greater extent which may support the energy demand for future generation.

Nomenclature

| | | | |
|-------------|---|-------------------|-----------------------------|
| A | area [m^2] | δ | Thickness [m] |
| C_p | heat capacity [$kJ/kg K$] | η | efficiency |
| D | diameter [m] | α_s | solar absorptivity |
| D_s | Outside diameter of the pipe [m] | β | collector tilt [$^\circ$] |
| d | depth of the honeycomb [m] | <i>Subscripts</i> | |
| \dot{E} | energy rate [kW] | <i>abs</i> | absorbed |
| F' | Collector efficiency factor [–] | <i>air</i> | air, ambient |
| F_R | heat removal factor [–] | <i>b</i> | bottom |
| G_{solar} | total solar irradiation [–] | <i>cp</i> | collector plate |
| h | heat transfer coefficient [W/m^2K] | <i>conv</i> | convective |
| I_T | incident solar energy per unit area of the absorber plate [Wm^{-2}] | <i>des</i> | destruction |
| K | thermal conductivity [$Wm^{-1}K$] | <i>f</i> | fluid |
| L | dimensions of the plate [m] | <i>gen</i> | generated |
| \dot{m} | mass flow rate [kg/s] | <i>gp</i> | glass plate |
| \dot{Q} | heat energy rate [kW] | <i>hc</i> | honeycomb |
| \dot{S} | entropy rate [kW/K] | <i>in</i> | input |
| S_r | radiation absorbed flux per unit area of absorber plate [Wm^{-2}] | <i>l</i> | loss |
| T | temperature [K] | <i>lk</i> | leaked |
| W | pitch of the tube [m] | <i>out</i> | output |
| w | honeycomb cell width [m] | <i>p</i> | plate |

| | | | |
|----------------------|---|------|--------------|
| \dot{X} | exergy rate [kW] | s | surface |
| Z | vertical height from the reference [m] | sd | stored |
| <i>Greek symbols</i> | | st | storage tank |
| ε | Emissivity [–] | t | top |
| σ | Stefan-Boltzmann constant [$Wm^{-2}K^{-4}$] | wp | water pipe |
| $\tau\alpha$ | effective product transmittance–absorptance | | |

References

- [1] Suzuki, A., A Fundamental Equation for Exergy Balance on Solar Collectors, *J. Sol. Energy Eng.*, 110 (1988), 2, pp. 102–106
- [2] Gupta, D. K. K., Saha, S. K., Energy Analysis of Solar Thermal Collectors, *J. Renew. Energy & Environ.*, (1990), pp. 283–287
- [3] Luminosu, I., Fara, L., Determination of the Optimal Operation Mode of a Flat Solar Collector by Exergetic Analysis and Numerical Simulation, *Energy*, 30 (2005), 5, pp. 731–747
- [4] Farahat, S., Sarhaddi, F., Ajam, H., Exergetic Optimization of Flat Plate Solar Collectors, *Renew. Energy*, 34 (2009), 4, pp. 1169–1174
- [5] Jafarkazemi, F., Ahmadifard, E., Abdi, H., Energy and Exergy Efficiency of Heat Pipe Evacuated Tube Solar Collectors, *Therm. Sci.*, 20 (2016), 1, pp. 327–335
- [6] Zhong, G., Huitao, W., Hua, W., Songyuan, Z., Xin, G., Exergy Analysis of Flat Plate Solar Collectors. *Entropy*, 16 (2014), 5, pp. 2549–2567
- [7] Sivaraman, G., Mohan, R., Harikrishnan, V., Experimental Investigation on Effect of Modified Solar Collector in Solar Water Heating System, *Therm. Sci.*, 24 (2020), 1, pp. 481–485
- [8] Malvi, C. S., Gupta, A., Gaur, M.K., Crook, R., Dixon, H. D. W., Experimental Investigation of Heat Removal Factor in Solar Flat Plate Collector for Various Flow Configurations, *Int. J. Green Energy*, 14 (2017), 4, pp. 442–448
- [9] Orlando, M. M., José, J. F. P., Heat Removal Factor in Flat Plate Solar Collectors: Indoor Test Method, *Energies*, 11 (2018), 10, pp. 2783
- [10] Hollands, K. G. T., Honeycomb Devices in Flat Plate Solar Collectors, *Solar Energy Society Conference, Phoenix Arizona, 1965*, Vol. 9, pp.159 -164
- [11] Mozumder, A Anjani K. S., and Sharma, P., Study of Cylindrical Honeycomb Solar Collector, *J. Sol. Energy*, 2014 (2014), pp. 7
- [12] Abdullah, A, H., Abou-Ziyan, H. Z., Ghoneim, A. A., Thermal Performance of Flat Plate Solar Collector using Various Arrangements of Compound Honeycomb, *Energy Convers. Manag.*, 44 (2003), 19, pp. 3093–3112
- [13] Dincer, I., Cengel, Y. A., Energy, Entropy and Exergy Concepts and Their Roles in Thermal Engineering, *Entropy*, 3 (2001), 3, pp. 116–149
- [14] Hottel, H. C., Keller, J. D., Effect of Reradiation on Heat Transmission in Furnaces and Through Openings, *Trans. A.S.M.E.*, 55 (1933), 55–56, pp. 39–49
- [15] Sukhatme, S. P., *Solar Energy*, McGraw-Hill., New York, USA, 2014
- [16] Najian, M. R., Exergy Analysis of Flat Plate Solar Collector, M. S. Thesis, Tehran University, Tehran, Iran, 2000

Submitted: 30.5.2020.

Revised: 28.10.2020.

Accepted: 12.11.2020